DEVELOPMENT OF PRESSURE REGAIN UNITS TO INCREASE EFFICIENCY OF FREE-RUNNING RADIAL FANS

Philipp OSTMANN, Dimitrios PETROU,
Martin KREMER, Dirk MÜLLER

RWTH Aachen University, Institute for Energy Efficient Buildings and Indoor Climate, Mathieustraße 10, 52074 Aachen, Germany

SUMMARY

Modern air handling units are usually equipped with free-running radial fans, that are mounted in an open air duct. Depending on the fan's operating point a significant amount of the energy is present in the form of dynamic pressure at the exit of the impeller. This paper investigates the implementation of additional flow guiding bodies (pressure regain units) downstream of a radial fan, to enhance the conversion of dynamic into static pressure, since dynamic pressure is usually treated as a loss when rating fan performance. It is found, that such pressure regain units are able to recover a substantial amount of static pressure and can therefore lead to an increase of the total-to-static fan efficiency.

INTRODUCTION

To meet the rising requirements of providing fresh air into offices or other non-residential buildings it is necessary to equip buildings with ventilation systems. Such a ventilation usually consists of a distribution system made up of several air ducts and an – in most cases central - air handling unit (AHU). Modern AHUs are usually equipped with backward-curved radial fans to provide the needed pressure increase and efficiency. Radial fans are mounted either in a spiral housing or in a free-running configuration, of which the latter is frequently found in central AHUs and therefore investigated in this study. By definition of the efficiency the fans are rated by their ability to provide a certain air volume flow at a certain total-to-static pressure increase. Since the static pressure does not include any kinetic parts, these are treated as loss. Hence, in order to achieve a maximum efficiency, it is required to convert as much dynamic pressure into static pressure. While a spiral housing fulfils this requirement quite well, a free-running configuration is prone to not being able to convert significant fractions of dynamic into static pressure [3].

This study first gives a brief look on the flow conditions downstream of a free-running radial fan and then presents the implementation of additional flow guiding geometries - so-called pressure regain units (PRU) - into the air duct channel. All investigations are performed with 3D numerical flow simulations.

NUMERICAL FLOW MODEL

Characteristic numbers

To characterize the performance of fans the measured values like volume flow, pressure increase and consumed power can be transformed into dimensionless numbers. The dimensionless numbers enable a comparison of the performance independent of the impeller diameter D and speed n. [2]
The flow coefficient φ relates the volume flow to the circumferential velocity at the impeller diameter.

$$\varphi = \frac{\dot{V}}{\frac{\pi^2}{4} D^3 n} \tag{1}$$

The pressure coefficient Ψ relates the total-to-static pressure rise to the dynamic pressure at the impeller exit.

$$\Psi_{ts} = \frac{\Delta p_{ts}}{\frac{\pi^2}{2} \rho D^2 n^2} \tag{2}$$

The power of the fan is calculated with the required torque at the impeller and the angular velocity and then related to the product of circumferential velocity and dynamic pressure at the impeller exit. This yields the power coefficient λ.

$$\lambda = \frac{P_{Fan}}{\frac{\pi^4}{8} \rho D^5 n^3} = \frac{M_{Fan} \cdot \omega}{\frac{\pi^4}{8} \rho D^5 n^3} \tag{3}$$

The total-to-static efficiency can be expressed by these three coefficients, which also leads to the widely known definition of fan efficiency.

$$\eta = \frac{\dot{V} \cdot \Delta p_{ts}}{M_{Fan} \omega} = \frac{\dot{V} \cdot \Delta p_{ts}}{P_{Fan}} \tag{4}$$

Recirculation flow leading to reduced efficiency

Figure 1 shows the flow field of the free running radial fan. The fan is operated at $2400\,\mathrm{min}^{-1}$ and $1450\,\mathrm{m}^3\,\mathrm{h}^{-1}$, which is near maximum efficiency at that speed. The left part of the figure shows the velocity magnitude. The high velocities at the impeller exit are clearly visible, while in fact the whole region around the impeller shows high velocities. The right part of the figure shows only the velocity component in z-direction with clipped positive values. With this approach, the areas where recirculation occurs can be clearly identified. As one could expect, there are two major regions. The smaller region is located in the corners of the mounting wall and it is driven partly by the fan gap flow. The more prominent region is downstream of the impeller. It is driven by the high momentum flow exiting the impeller.
Based on these observations, one can sketch the typical flow field downstream of a free-running radial fan as in Figure 2. In this study the large recirculation region downstream the impeller and engine is targeted.
Azem, A. et al. [1] indicate an additional body in that area as beneficial for pressure increase and therefore efficiency of a ventilation system. In their work, they showed that improvements by up to 10 % can be achieved, if a PRU is implemented. Since they only investigated rather simple, cuboid shapes, further improvements are deemed possible, when more sophisticated, diffusor-like shapes are implemented.

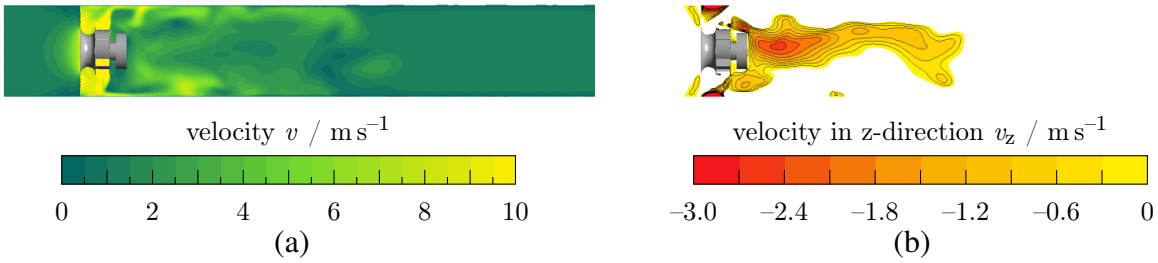

Figure 1: Flow field of the free-running radial fan at 2400 min^{-1} and 1450 m^3 h^{-1} in its base configuration.

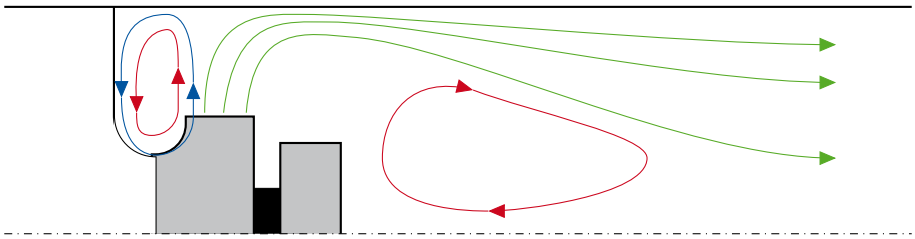

Figure 2: Sketch of potentially scavengous flows in an open air duct channel.

Geometry and boundary conditions

To perform the numerical flow calculations the commercial software *ANSYS CFX 20.2* is used. The geometry is designed with *DesignModeler*, which is part of the *ANSYS Workbench* package. Since the focus of this study is to investigate the influence of additional bodies downstream of the fan, a rather simple generic fan geometry is designed. The important geometrical parameters are sketched in Figure 3. The fan is mounted in a square air duct and is equipped with a simplified inlet nozzle. The radial gap is also modelled, although not in detail. To predict the flow field downstream of the fan more accurately, the engine and the engine shaft are implemented in a simplified manner.
The impeller is implemented using the so-called "frozen-rotor approach". In addition to the inner rotating impeller-region which includes the fan blades, the surrounding impeller surfaces are implemented as rotating walls. The engine shaft and the engine itself are treated stationary. As for the engine shaft its influence was deemed rather small, leading to this decision. As inlet condition a massflow condition is chosen. The required massflow is calculated by the required volumeflow and air density at the inlet. The outlet conidition is represented by a static pressure condition, set at 0 Pa over the reference pressure of 1 bar. The outlet boundary condition is positioned approximately 4.5 m downstream of the impeller. Additionally two evaluation planes are implemented immediately upstream and downstream the PRU. In combination with the evaluation at the impeller exit interface,

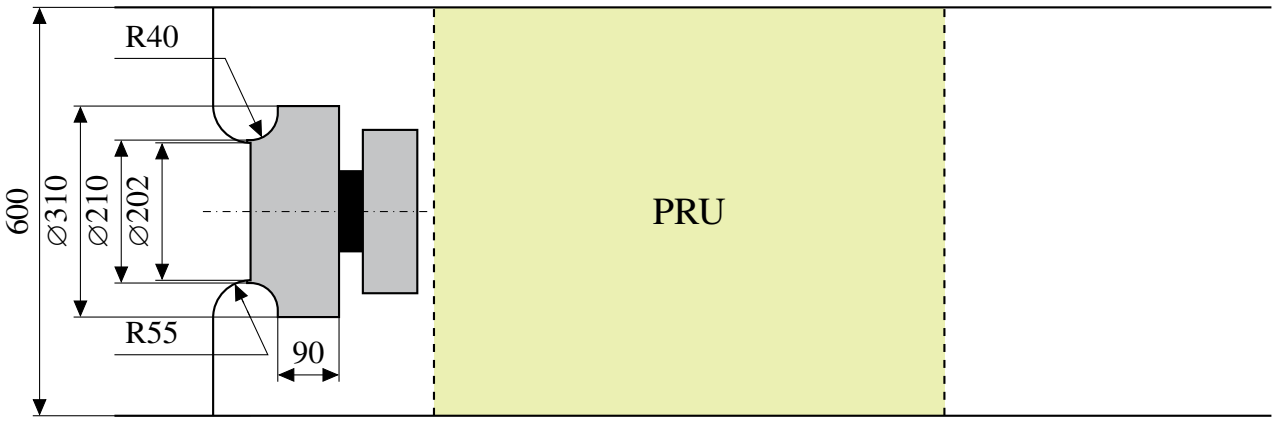

Figure 3: Overview of the modelled geometry.

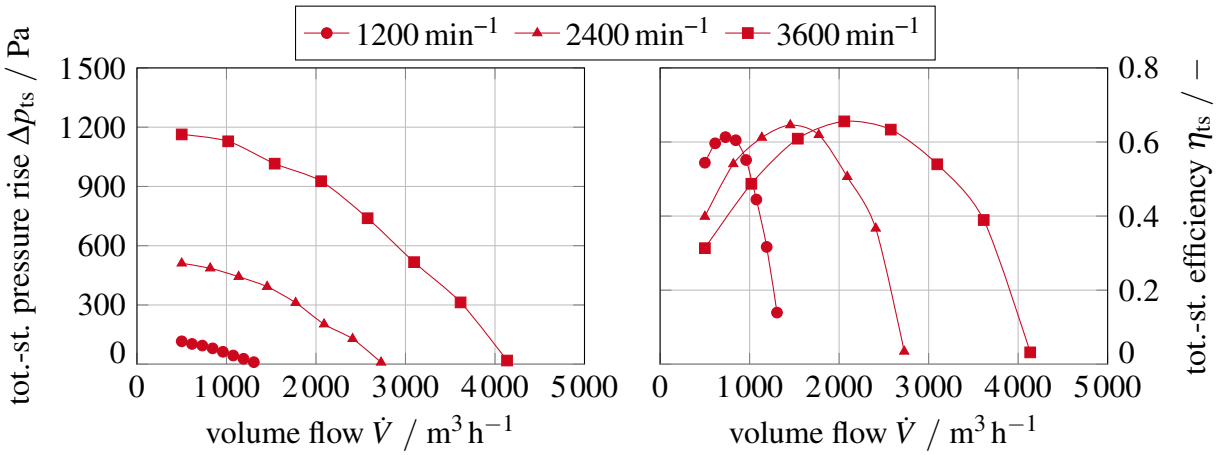

Figure 4: Performance maps of the configuration without a pressure regain unit (base configuration).

the relevant values can be reported at five positions.
This setup allows to predict the swirl-afflicted flow field inside the impeller and downstream of it.
The required mesh is generated in ANSYS Meshing and consists of tetrahedral cells and inflation layers on the important surfaces. The mesh consists of roughly 2.0 – 2.4 $\times$ 10^6 cells - depending on the PRU design - with a maximum size of 10 mm everywhere upstream of the exit of the PRU region. The impeller itself is refined with a maximum cell size of 3 mm.
The performance map of the empty channel configuration cases, shown in Figure 4, determines the operating point distribution for all other configurations. Three fan speeds are investigated and each speed line consists of eight equally distributed operating points. The minimum volume flow is set to 500 m^3 h^{-1} for all configurations and the maximum volume flow is defined by a total-static pressure increase near 10 Pa to prevent negative values. The acquired operating points, consisting of volume flow and fan speed, are then applied to all other configurations.
The global performance metrics like total-static pressure increase and efficiency are evaluated with the values at in- and outlet of the calculation domain. To rate the performance of the PRU designs a pressure regain ratio is introduced that relates the static pressure increase to the decrease of dynamic pressure. A higher value indicates a better conversion of kinetic energy into static pressure.

$$\chi = \frac{p_{st,2} - p_{st,1}}{p_{dyn,1} - p_{dyn,2}} \tag{5}$$

The ratio is evaluated for the PRU itself (index “PRU”) and for the impeller exit and domain outlet (index “total”), yielding two slightly different values. Due to the geometrical extent of the PRU designs 3.1 – 3.3 (see Table 1, Figure 5) only the total value is reported for these configurations. Since some static pressure is regained for the empty channel configuration as well, the pressure regain ratio is reported as well.
All operating points are calculated with at least 2000 iterations and until either, the deviation of the total-static pressure increase and the efficiency is within a specified tolerance gap or a maximum of 4000 iterations is reached. Additionally, all reported values are averaged arithmetically over the last 100 iterations.

Development of PRU shapes

We consider the proposed PRU shape by Azem, A. et al. [1] as baseline design with a simple cuboid-like geometry approach. In contrast to their found optimum, we keep the PRU shorter to be more flexible in the other designs. It is expected, that it will perform worse than what they found. All PRU configurations are sketched in Figure 5. The different shapes are differently coloured to indicate the design process. To enhance the pressure regain abilities an additional diffusor shape is extended

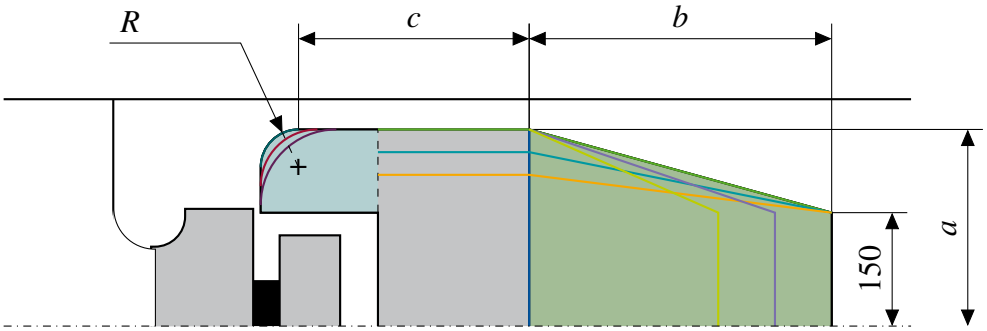

Figure 5: Sketch of the different PRU designs.

Table 1: Overview of geometry parameters of the designed PRUs

	a - mm	**b - mm**	**c - mm**	**R - mm**
0.0	-	-	-	-
1.0	260	-	200	-
2.1	260	400	200	-
2.2	230	400	200	-
2.3	200	400	200	-
2.4	260	325	200	-
2.5	260	250	200	-
3.1	260	400	245	100
3.2	260	400	270	75
3.3	260	400	295	50

downstream (green part in Figure 5). The second enhancement aims at a better flow guidance into the PRU section by extending the PRU upstream and blending the edges (blue part in Figure 5).
The corresponding geometrical lengths are summarized in Table 1. For designs 1.0 and 2.1, we designed the gap area between PRU and air duct wall to be approximately the same as the exit area of the impeller. The designs 2.1 - 2.5 aim at optimizing the diffusor shape in respect to length and total cross sectional area of the PRU. To investigate the influence of the inflow, the designs 3.1 - 3.3 originate from the dimensions used for design 2.1.

RESULTS

Although the simulations were performed as steady state simulations, the underlying physics are strongly time-dependent. Especially the rotating impeller would produce periodic fluctuations due to the rotating blades. By using the frozen-rotor approach the swirl is resolved and its influence is implicitly included in the presented results. The underlying unsteady physics lead to some irregularities of the flow fields, which are captured at the last iteration. To comprehend the influence of the PRUs, it is necessary to discuss two important effects.
The first effect is the reduction of turbulent losses, which are characterized by turbulent shear flows that dissipate energy and therefore reduce the kinetic energy. To quantify the amount of turbulent

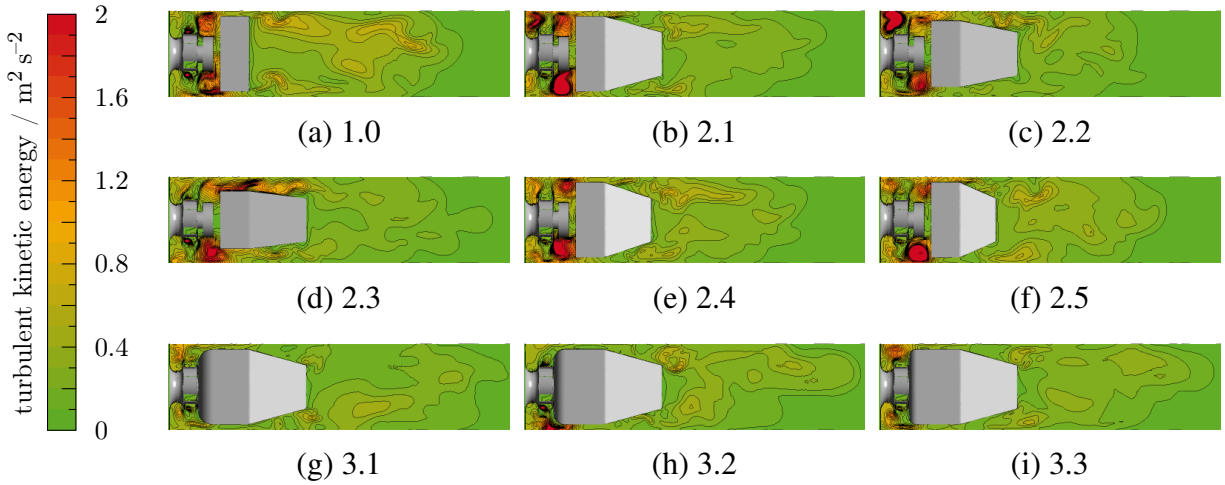

Figure 6: Contours of the turbulent kinetic energy for all PRU designs for at 2400 min^{-1} and 1450 $m^3\,h^{-1}$.

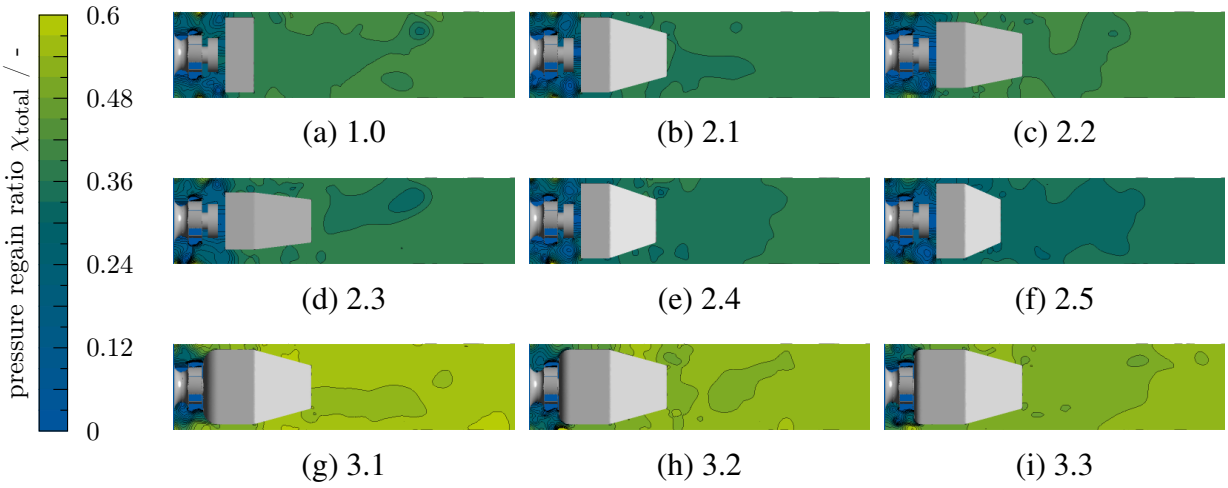

Figure 7: Contours of the pressure regain ratio for all PRU designs for at 2400 min^{-1} and 1450 $m^3\,h^{-1}$.

flow we investigate the turbulent kinetic energy (TKE), which is a direct result of the conducted flow simulations. In general, areas with a high amount of TKE will also cause higher aerodynamic losses. In order to improve the efficiency, the overall amount of TKE and the size of areas with high TKE should be reduced. In Figure 6, contours of the TKE are shown for all PRU designs. When comparing design 1.0 to the 2.x designs a reduction of TKE is visible in the downstream area, while there are still problematic areas upstream the PRU. With the 3.x designs it is possible to reduce those areas significantly as well. Only design 3.2 shows an anomalous amount of TKE just at the PRU entry. This is the case for the whole operating range, leading to a decreased efficiency for this design. The exact cause for this phenomenon needs an investigation in more detail.

The second effect is the ability to convert dynamic into static pressure. In Figure 7, the contours of the pressure regain ratio are shown. The definition (see eq. 5) is slightly altered, as the static pressure at the respective location is used for $p_{st,2}$.

To complement the primarily visual comparison in Figure 7, the development of the total, static and dynamic pressure is shown in Figure 8 for three operating points. The total pressure loss is reduced for every PRU design, while the reduction is strongest for the 3.x designs. For lower volume flows, the regain of static pressure occurs almost exclusively upstream of the *PRU Out* position, indicating negligible losses downstream the position. The 3.x designs are able to achieve their respective pressure regain upstream of *PRU In*, indicating that the inflow has the biggest impact. With rising volume

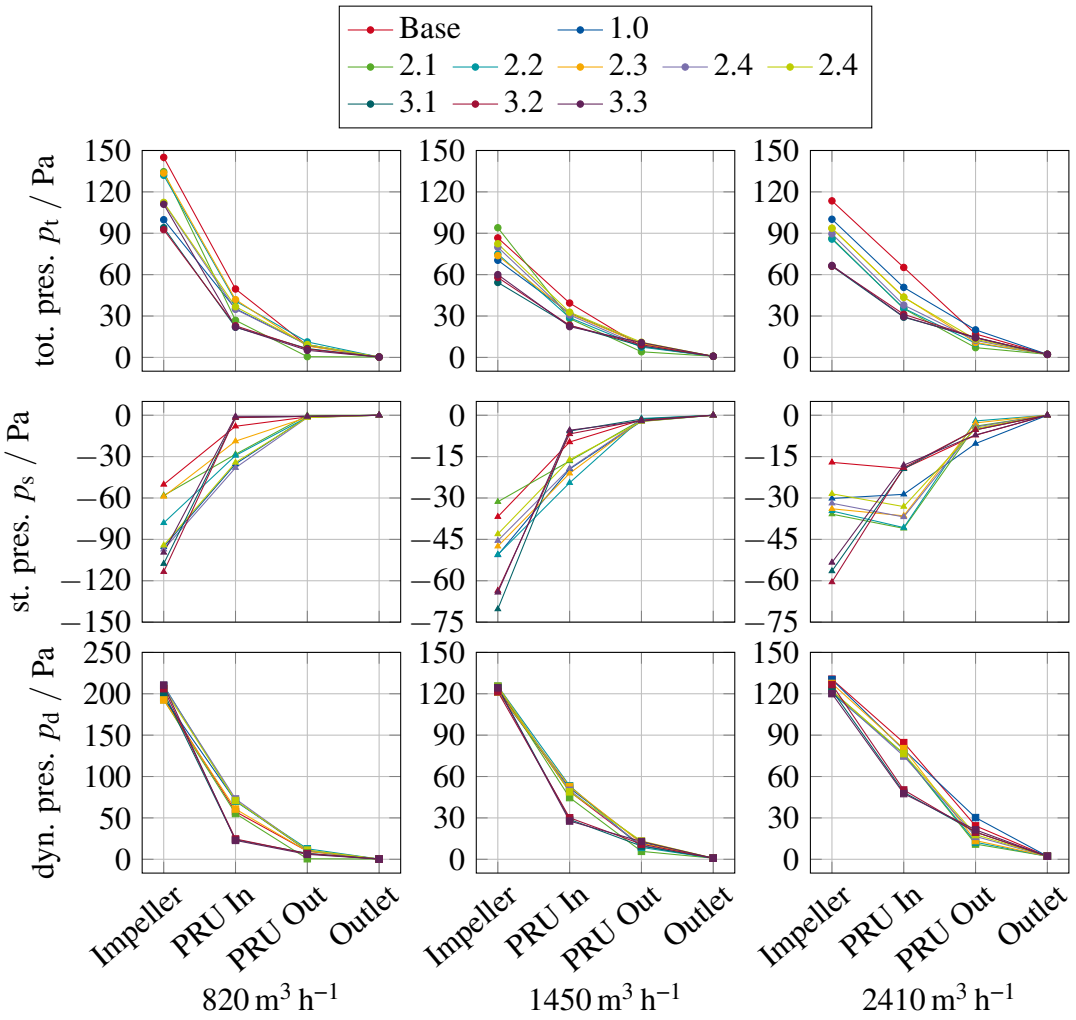

Figure 8: Pressure development of the various PRU designs for 2400 min^{-1}.

flows the downstream portion (after *PRU In*) of the 3.x PRUs gains contribution to the pressure regain. In Figure 9 an overview of all calculated pressure regain ratios is given. As expected, an empty channel only achieves small pressure regain ratios of about 30 %. When adding the rather simple PRU 1.0, this value rises up to about 50 %. But due to strong fluctuations in the downstream field of the PRU, the value as well fluctuates strongly over the operating range. The volume flow impacts all 2.x designs as well, although they are much more stable over changing fan speeds. Only for lower volume flows, the 1.0 design is superior to some 2.x designs. For higher volume flows, design 2.2 performs the best out of all 2.x designs. For lower volume flows, a shorter PRU like 2.4 or 2.5 tends to perform better, since the influence of a sharper diffusor angle is less impactful.
The additional inflow blending of the 3.x designs nearly eliminates the influence of the volume flow and a minimum pressure regain ratio of nearly 50 % is achieved over the whole operating range.
To summarize the influence of the PRUs on the total-static efficiency, the corresponding values are reported in Figure 10. The left plot shows the flow coefficient interval in which each configuration achieves an efficiency above 60 %. Additionally the flow coefficient with the maximum efficiency is marked approximately. The right plot shows the corresponding maximum efficiency values.
In nearly all cases maximum efficiency is achieved at a flow coefficient of approximately 0.13 - 0.15, while there is a tendency towards lower flow coefficients with rising fan speed. The maximum achievable efficiency rises with growing fan speed, although the gain is stronger at lower fan speeds. While PRU 1.0 only allows for a moderate increase of efficiency, the additional diffusor shape of the 2.x designs raises the efficiency by up to 7 %-pts compared to the base configuration. The geometry pa-

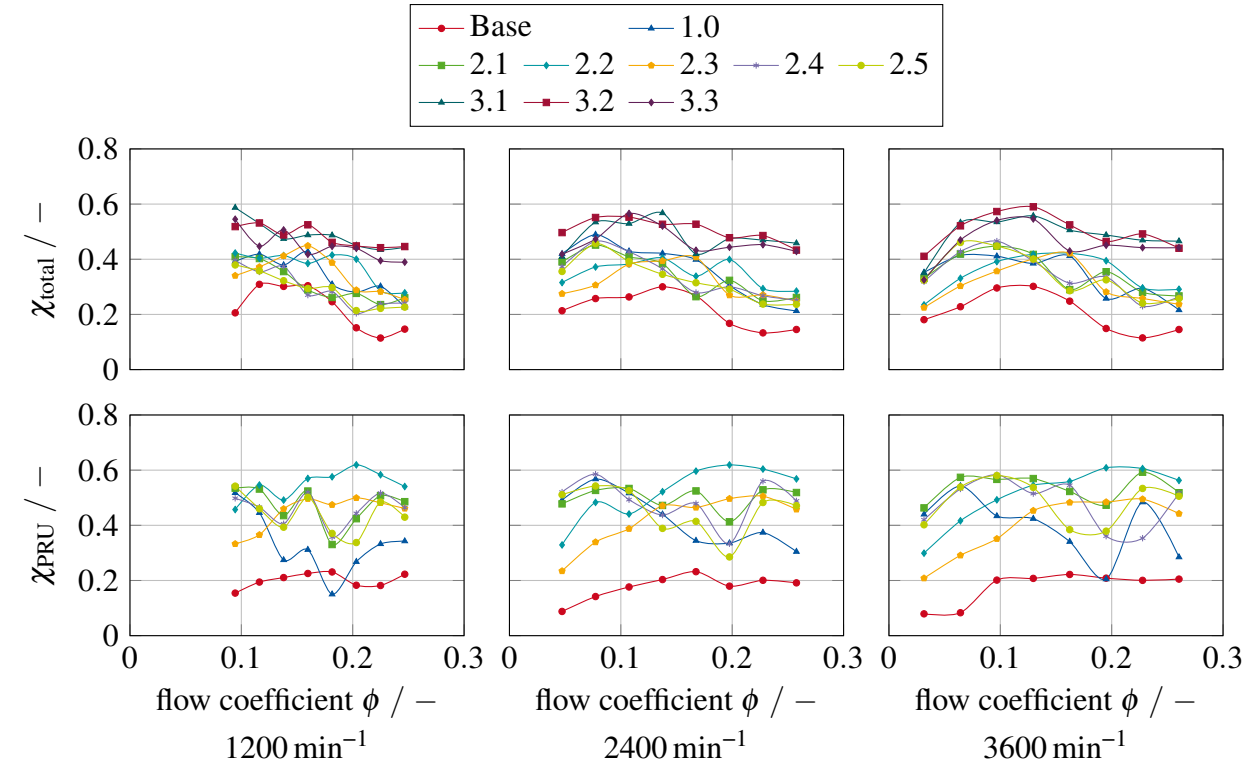

Figure 9: Pressure regain ratios of the PRU designs.

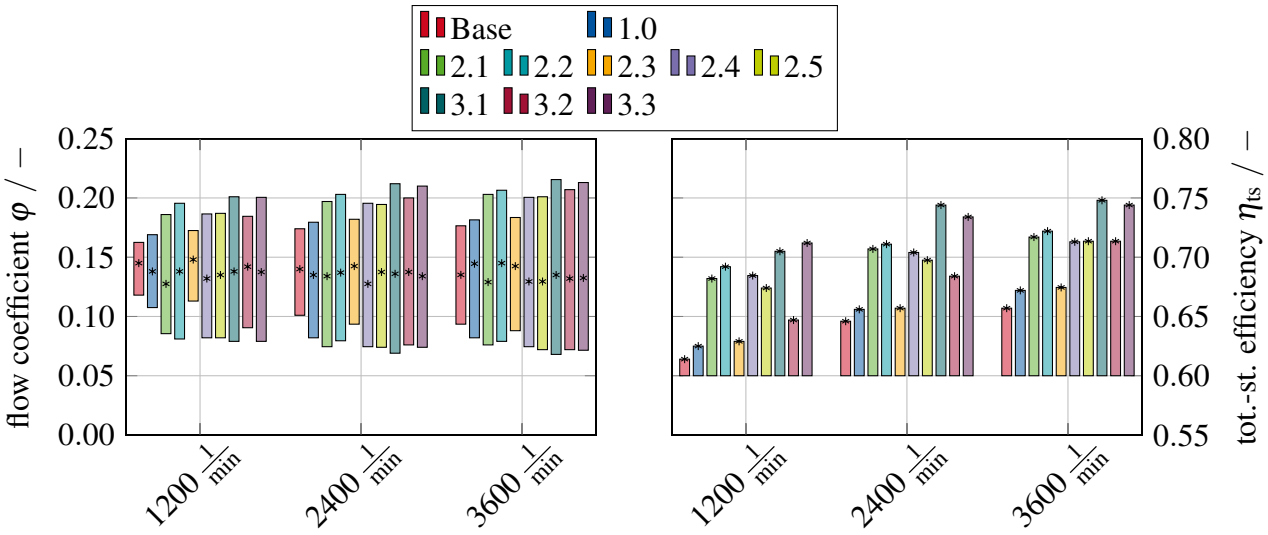

Figure 10: Overview of the achieved efficiencies for the various PRU designs.

rameter a has a strong influence on the results. If the PRU is designed too slim, the efficiency drops. Length c should not fall below a certain value, since otherwise the diffusor angle becomes too sharp and therefore leads to increased losses. If the PRU entry is designed with an additional blending, further increases are possible. It appears that the radius R should be maximized, but overall the influence is quite small compared to the blending of the inflow at all. Design 3.1 increases the efficiency by up to 13 %-pts compared to the base configuration.

CONCLUSION

By achieving an overall less turbulent flow downstream the free-running radial fan and implementing a diffusor-like shape, the presented PRU designs are able to contribute to a significant enhancement in static pressure increase and therefore efficiency improvements. The results are to be validated by experiments, but the presented work offers guidelines to design prototypes and their expected performance. An ideal design should consist of a rounded inflow geometry, which is followed by a diffusor with a moderate diffusor angle. An additional optimization of the smaller recirculation regions at the fan-mounting wall is still to be investigated as well.
Since the flow was shown to be less turbulent, the acoustic behaviour is expected to be better as well. For further enhancenment, the PRUs could be manufactured with noise absorbing material, to achieve a better noise damping.

BIBLIOGRAPHY

[1] Azem, A., Mathis, P., Stute, F., Hoffmann, M., Müller D. and Hetzel, G. Efficiency increase of free running centrifugal fans through a pressure regain unit used in an air handling unit. *Energy and Buildings*, pages 321–327, 2018.

[2] Carolus, T. *Ventilatoren - Aerodynamischer Entwurf, Schallvorhersage, Konstruktion*. Springer Vieweg, 2013.

[3] Ratter, H., Caglar, S. and Gabi, M. Empirical model for the quantitative prediction of losses of radial fans based on CFD calculations. *Journal of Thermal Sciene*, pages 304–310, 2013.

ACKNOWLEDGEMENT

Grateful acknowledgement is made for financial support by BMWK (Federal Ministry for Economic Affairs and Climate Action), promotional reference 03ET1606B. Simulations were performed with computing resources granted by RWTH Aachen University under project rwth0460.